LU TP 02-09
NORDITA-2002-22 HE

# Center–Vortex Solutions of the Yang–Mills Effective Action in Three and Four Dimensions

Dmitri Diakonov[1,2] and Martin Maul[3]
[1] *NORDITA, Blegdamsvej 17, 2100 Copenhagen Ø, Denmark*
[2] *St. Petersburg Nuclear Physics Institute, Gatchina, St.Petersburg 188 300, Russia*
[3] *Department of Theoretical Physics, Lund University, Sölvegatan 14A, S - 223 62 Lund, Sweden*
(Dated: April 10, 2002)

We calculate the one-loop effective action of the $SU(2)$ Yang–Mills theory for center-vortex configurations, both in $3d$ and $4d$. We find that in both cases there are minima of the effective action, corresponding to vortices of the transverse size approximately $4/g_3^2$ and $1.7/\Lambda_{\overline{MS}}$, respectively. The values of the effective actions at the minima are *negative*, suggesting that the Euclidian vacuum may be unstable with respect to creation of vortices.

PACS numbers: 11.10.Lm, 11.15.Kc, 12.38.-t



## I. INTRODUCTION

Recently there have been certain indications from lattice simulations that center-of-group vortices [1] may be responsible for the area behavior of large Wilson loops, i.e. for confinement, see e. g. [2, 3, 4] and references therein. If long closed vortices populate the Euclidean vacuum of QCD, resembling curved and entangled spaghetti in Italian *pasta*, it might serve as a microscopic mechanism of confinement.

From the continuum side, however, vortices invoke more questions than there are answers today. First of all, there are no vortex-type solutions of the classical Yang–Mills equations. Therefore, vortices can at best arise as saddle points of the effective action, with quantum fluctuations about a trial vortex configuration taken into account. Second, if the effective action contains vortex configurations as saddle points, their energy per unit length in $3d$ or per unit surface in $4d$ should be either small positive or, even better, slightly negative. If it is large and positive there is no reason for the vortices to appear in the physical vacuum, in the first place. Third, the typical lengths where vortices bend to an angle of the order of unity must be on the average larger than the characteristic transverse size of the vortex. If it is not so, the fluctuation cannot be called a vortex. Fourth, different vortices in the vacuum or different segments of the same vortex need to be on the average repulsive so that they do not glue up. Ultimately, one has to build a consistent statistical mechanics of the vortex vacuum in order to see that the 'entangles spaghetti' have a preferred vacuum free energy as compared to, say, the instanton liquid. The statistical mechanics of instantons is quite a difficult problem by itself [5, 6], but vortices are far more difficult to deal with.

In this paper, we address the first and in fact the easiest questions from the above list. For vortices to be physical objects and not artifacts of a regularization and gauge fixing, their typical transverse sizes must be finite in physical units, i.e. to be of the order of $1/g_3^2$ in $3d$ and of the order of $1/\Lambda_{\rm QCD}$ in $4d$. Correspondingly, the energy of a vortex per unit length should be of the order of $g_3^2$ in $3d$, and the energy per unit surface should be of the order of $\Lambda_{\rm QCD}^2$ in $4d$. The appearance of $\Lambda_{\rm QCD}$ implies the transmutation of dimensions through renormalization; it can be achieved only with quantum fluctuations about the vortex taken into due account. We study here the effective action with quantum fluctuations about a trial vortex configuration being integrated out, at the one-loop level. Although the one-loop approximation is not the whole story, it is the first attempt to find out if there are any hints from the continuum Yang–Mills theory that 'thick' vortices have the right to exist. We seem to get a positive answer to this question.

In what follows, we consider an idealized isolated infinitely long and straight vortex perpendicular to the $(xy)$ plane. We choose an Ansatz for the vortex profile in the transverse plane $\bar{A}_\mu(x,y)$ and expand the YM action into the classical part, $\int d^dx F_{\mu\nu}^2(\bar{A})/4g_d^2$, and the part quadratic in the fluctuations $a_\mu$ about the background $\bar{A}_\mu$. Integration over $a_\mu$ (and over ghost fields stemming from background gauge fixing) is then performed using the scattering theory methods; it results in the quantum part of the effective action. The full effective action is the sum of the classical and quantum parts. In fact, we study several functional forms of the profile and find that in each case there exists a minimum of the action with respect to the transverse spread of the vortex. It turns out to be about $(4-5)/g_3^2$ in $3d$ and about $(1.6-1.8)/\Lambda_{\overline{MS}}$ in $4d$. The values of the effective action at the minima are *negative* in all cases considered. It indicates that the Yang–Mills vacuum might be unstable in regard to the spontaneous production of vortices.

## II. THE VORTEX ANSATZ

By definition of a $Z(N)$ vortex, the Wilson loop in the fundamental representation of the $SU(N)$ gauge group, winding around the vortex in the transverse plane assumes values being nontrivial elements of the group center, as the radius of the Wilson loop tends to $\infty$:

$$\mathrm{P}\exp i\oint A_\mu dx^\mu \to \begin{pmatrix} e^{2\pi ik/N} & & \\ & \ldots & \\ & & e^{2\pi ik/N} \end{pmatrix} \in Z_N, \tag{1}$$

where $k = 1, \ldots, N-1$. In this paper, we consider the $SU(2)$ gauge group (although we also make calculations in $SU(3)$ for additional checks). In $SU(2)$ the only nontrivial element of the center is the minus unity $2\times 2$ matrix. Taking for example a circular Wilson loop of radius $\rho$ in the $(xy)$ plane around a vortex centered at $\rho = \sqrt{x^2+y^2} = 0$ we see that only the azimuthal component of the Yang–Mills field is involved in eq. (1), $A^a_\phi = \epsilon_{\alpha\beta}n_\alpha A^a_\beta$, where $n_\alpha$ is a unit vector in the $(xy)$ plane. One can always choose a gauge where $A_\phi$ is independent of the azimuthal angle $\phi$. Generally speaking, it implies that the radial component $A_\rho$ is nonzero, however, we shall neglect this component as the condition (1) is compatible with $A_\rho = 0$. If $A_\rho$ is nonzero it can be reconstructed from gauge invariance by replacing $\partial_\rho \to \partial_\rho\delta^{ab} + f^{acb}A^c_\rho$. A circular Wilson loop in the $J = \frac{1}{2}$ representation lying in the transverse plane and surrounding the vortex center is [7]:

$$W_{\frac{1}{2}}(\rho) = \frac{1}{2}\mathrm{Tr}\ \mathrm{P}\exp i\oint \rho A^a_\phi t^a d\phi = \cos[\pi\mu(\rho)], \qquad \mu(\rho) = \rho\sqrt{A^a_\phi(\rho)A^a_\phi(\rho)}, \tag{2}$$

For an arbitrary representation of $SU(2)$, labeled by spin $J$, one has:

$$W_J(\rho) = \frac{1}{2J+1}\frac{\sin[(2J+1)\pi\mu(\rho)]}{\sin[\pi\mu(\rho)]}. \tag{3}$$

If $\mu(\rho)$ tends to an odd integer at large $\rho$, the Wilson loop $W_J(\rho) \to (-1)^{2J}$. For half-integer representations it is minus unity, hence $\mu(\infty) = 2n+1$ is the condition that one deals with a $Z(2)$ vortex. We shall only consider the case when $\mu(\infty) = 1$. For simplicity we assume that only one color component of $A_\phi$ is nonzero:

$$\bar{A}^a_\phi(\rho) = \delta^{a3}\frac{\mu(\rho)}{\rho}, \qquad \mu(0) = 0, \qquad \mu(\infty) = 1, \tag{4}$$

where $\mu(\rho)$ will be called the profile of the vortex. Eq. (4) with all the rest components of the YM field set to zero, is the Ansatz for the center vortex field we are going to investigate.

## III. THE CLASSICAL ACTION OF THE VORTEX

We take an idealized straight-line (in $3d$) or straight-surface (in $4d$) vortex whose dimension in the longitudinal direction is $L_{||}^{(d-2)}$ ($d = 3, 4$), while in transverse plane it has a trial profile $\mu(\rho)$. The classical action of the vortex is (see Appendix A):

$$S_{\mathrm{class}} = \frac{1}{4g_d^2}\int d^dx (F^a_{\mu\nu})^2 = \frac{1}{2g_d^2}\int d^{d-2}x_{||}\int d^2x_\perp\, (B^a_{||})^2$$

$$= L_{||}^{(d-2)}\,\frac{\pi}{g_d^2}\int_0^\infty d\rho\,\rho\left[\frac{1}{\rho}\partial_\rho(A^a_\phi\rho)\right]^2 = L_{||}^{(d-2)}\,\frac{\pi}{g_d^2}\int_0^\infty d\rho\rho\left[\frac{1}{\rho}\frac{\partial}{\partial\rho}\mu(\rho)\right]^2 \equiv L_{||}^{(d-2)}\mathcal{E}_{\mathrm{class}}\,. \tag{5}$$

We remind the reader that in $3d$ the coupling constant $g_3^2$ has the dimension of mass, and the theory is convergent. In $4d$ the (bare) coupling $g_4^2$ is dimensionless but gets an infinite renormalization from quantum fluctuations. To the one-loop accuracy one can parameterize:

$$\frac{8\pi^2}{g_4^2} = \frac{11}{3} N \ln \frac{M}{\Lambda_{\rm QCD}} , \tag{6}$$

where $M$ is the ultra-violet cutoff in a particular regularization scheme. The quantum part of the effective action is logarithmically divergent; the renormalizability of the theory ensures that the dependence on the UV cutoff $M$ is canceled in the full effective action.

## IV. DIMENSIONAL ANALYSIS

Let us make a quick estimate of the 'best' transverse size of the vortex $\rho_0$ from a simple dimensional analysis. We denote the action per unit longitudinal dimension of the vortex by $\mathcal{E}$ such that $S = L_{||}^{(d-2)}\mathcal{E}$, and call $\mathcal{E}$ the transverse energy of the vortex. If $\rho_0$ is the scale of the profile function $\mu(\rho)$ [e.g. $\mu(\rho) = \exp(-\rho_0/\rho)$], we find on dimensional grounds that in $4d$

$$\mathcal{E}_{\rm class} = \frac{A}{\rho_0^2} \frac{11\,N}{24\pi^2} \ln \frac{M}{\Lambda_{\rm QCD}}, \tag{7}$$

where $A$ is the dimensionless functional of the trial profile,

$$A = \pi\rho_0^2 \int_0^\infty \frac{d\rho}{\rho} \left(\frac{d\mu}{d\rho}\right)^2 . \tag{8}$$

The renormalizability ensures that the quantum part of the effective action has exactly the same coefficient in front of the divergent $\ln M$ piece, but with the opposite sign, so that $\ln M$ cancels in the sum of the classical and quantum parts:

$$\mathcal{E}_{\rm quant} = -\frac{A}{\rho_0^2} \frac{11\,N}{24\pi^2} \ln(M\rho_0 B), \qquad \mathcal{E}_{\rm eff} = \mathcal{E}_{\rm class} + \mathcal{E}_{\rm quant} = -\frac{A}{\rho_0^2} \frac{11\,N}{24\pi^2} \ln(\Lambda_{\rm QCD}\rho_0 B), \tag{9}$$

where $A, B$ are numerical coefficients depending on the concrete functional form of the profile $\mu(\rho)$. $\mathcal{E}_{\rm eff}$ has the minimum at

$$\rho_0^{\rm min} = \frac{\sqrt{e}}{\Lambda B}, \qquad \mathcal{E}_{\rm eff}^{\rm min} = -\Lambda^2 \frac{11\,N}{24\pi^2} \frac{AB^2}{2e}, \qquad e = 2.71828... \tag{10}$$

In $3d$ a similar dimensional analysis yields:

$$\mathcal{E}_{\rm class} = \frac{A}{g_3^2\rho_0^2}, \qquad \mathcal{E}_{\rm quant} = -\frac{C}{\rho_0}, \tag{11}$$

with the same coefficient $A$ as in $4d$. The sign of $C$ is apriori unknown. However, since the theory is super-renormalizable one expects that the sign of the quantum energy is the same as in $4d$ at $M\bar{\rho} \to \infty$, i.e. negative (direct calculations below confirm the expectation). The sum $\mathcal{E}_{\rm eff} = \mathcal{E}_{\rm class} + \mathcal{E}_{\rm quant}$ has then a minimum at

$$\rho_0^{\rm min} = \frac{1}{g_3^2} \frac{2A}{C}, \qquad \mathcal{E}_{\rm eff}^{\rm min} = -g_3^2 \frac{C^2}{4A}. \tag{12}$$

Notice that both in $3d$ and $4d$ we get a natural result for the transverse size of the vortex and a *negative* sign for its transverse energy at the minimum.

In a sense we have already proven the main statements of the paper put in the Abstract and the Introduction: these statements follow from dimensional analysis and the renormalizability of the theory. However, one still needs to compute the numerical coefficients $A, B, C$ and look for the best profile function $\mu(\rho)$, and that is what the rest of the paper is about.

## V. THE QUANTUM ACTION ABOUT A VORTEX

### A. Definition of the quantum action

To get the quantum action for $\mu(\rho)$ we integrate over quantum fluctuations about a given background field $\bar{A}^a_\phi(\rho)$ (see eq. (4)) considered to be a slowly varying field with momenta $k_\perp$ up to certain $k_{\rm min}$. Accordingly, quantum fluctuations have momenta $k_\perp$ above $k_{\rm min}$ and arbitrary longitudinal momenta. Writing $A_\mu = \bar{A}_\mu + a_\mu$ we expand $F^2_{\mu\nu}(A+a)$ in the fluctuation field $a_\mu$ up to the second order appropriate for the 1-loop calculation. The term linear in $a_\mu$ vanishes due to the orthogonality of high and low momenta and also because $\bar{A}_\mu$ is in our case independent of $\phi$ and longitudinal coordinates whereas $a_\mu$ is dependent on those coordinates.

The quadratic form for $a_\mu$ is the standard (see e.g. [8])

$$W^{ab}_{\mu\nu} = -[D^2(\bar{A})]^{ab}\delta_{\mu\nu} - 2f^{acb}F^c_{\mu\nu}(\bar{A}), \tag{13}$$

if one imposes the background Lorentz gauge condition,

$$D^{ab}_\mu(\bar{A})a^b_\mu = 0, \qquad D^{ab}_\mu(\bar{A}) = \partial_\mu\delta^{ab} + f^{acb}\bar{A}^c_\mu. \tag{14}$$

The quantum part of the effective action is, as usually, given by the small-oscillation determinants:

$$S_{\rm quant}[\bar{A}] = S_{\rm gluon} + S_{\rm ghost} = \frac{1}{2}\ln\det(W^{ab}_{\mu\nu}) - \ln\det(-D^2_\mu). \tag{15}$$

Subtraction of free determinants (with zero background field) is understood.

The full effective action is $S_{\rm eff} = S_{\rm class} + S_{\rm gluon} + S_{\rm ghost}$. Since all terms are proportional to the longitudinal dimensions of the vortex $L_{||}^{(d-2)}$ we shall divide all terms by this quantity; it will then become an equation for the appropriate contributions to the transverse energy of the vortex,

$$\mathcal{E}_{\rm eff} = \mathcal{E}_{\rm class} + \mathcal{E}_{\rm gluon} + \mathcal{E}_{\rm ghost}, \tag{16}$$

where all terms are certain functionals of the trial vortex profile $\mu(\rho)$.

### B. The ghost operator

For the vortex Ansatz (4) the ghost operator $(D^2)^{ab}$ takes the following simple form in the cylindrical coordinates [7]:

$$D^2 = \left(\frac{1}{\rho}\frac{\partial}{\partial\rho}\rho\frac{\partial}{\partial\rho} + \partial_3^2 + \ldots\partial_d^2\right)\delta^{ab} + \frac{1}{\rho^2}\left(\delta^{ac}\frac{\partial}{\partial\phi} + f^{a3c}\mu(\rho)\right)\left(\delta^{cb}\frac{\partial}{\partial\phi} + f^{c3b}\mu(\rho)\right). \tag{17}$$

The eigenvalues of the structure constants $if^{a3c}$ in the color space are

$$\alpha_c = \begin{cases} \{0,1,-1\} & \text{for SU(2)}, \\ \{0,0,1,-1,1/2,1/2,-1/2,-1/2\} & \text{for SU(3)}. \end{cases} \tag{18}$$

It is natural to choose a plane wave basis $\exp(ik_{||}\cdot x_{||})$ for the longitudinal directions $x_3,\ldots x_d$, and a polar basis $\exp(im\phi)Z^{(c)}_m(\rho)$ for the transverse directions. The eigenfunctions $Z^{(c)}_m(\rho)$ satisfy the second-order differential equations depending on the color polarization $c = 1,\ldots,(N_c^2-1)$:

$$\left[-\frac{1}{\rho}\frac{\partial}{\partial\rho}\rho\frac{\partial}{\partial\rho} + \frac{(m-\alpha_c\,\mu(\rho))^2}{\rho^2}\right]Z^{(c)}_m(\rho) = k^2_{\perp\,cm}Z^{(c)}_m(\rho). \tag{19}$$

For each color polarization $c$ one has to solve a separate eigenvalue equation with a corresponding coefficient $\alpha_c$ from eq. (18). The spectrum in $k_\perp$ is continuous with the spectral density depending on $m$ and $c$. By putting the system into a large circular box of radius $R$, one makes the spectrum discrete, and the eigenvalues $k_\perp$ can be labeled by a discrete number $n$.

The eigenvalues of the full operator $-D^2$ are then

$$E^2(c,m,n,k_{||}) = k_{||}^2 + k_{\perp\, cmn}^2, \tag{20}$$

and one has to sum over the color polarizations labeled by $c$, the magnetic quantum numbers $m$, the radial quantum numbers $n$ and integrate over the continuous spectrum in $k_{||}$. In the free case ($\mu = 0$) the eigenfunctions of eq. (19) are the ordinary Bessel functions $J_{|m|}(k_{0\perp mn}\rho)$ (the index must be non-negative to ensure the regularity at the origin). In this case the eigenvalues $k_{0\perp mn}$ can be determined by the zeros of the Bessel functions.

According to eq. (15), the ghost contribution to the transverse energy of the vortex is the sum of logarithms of the eigenvalues:

$$\begin{aligned}\mathcal{E}_{\rm ghost} &= -\sum_{c,m,n,k_{||}} \left[\ln E^2(c,m,n,k_{||}) - \ln E_0^2(c,m,n,k_{||})\right] \\ &= -\sum_{c=1}^{N^2-1}\sum_{m=-\infty}^{\infty}\sum_{n}^{\infty}\int \frac{d^{d-2}k_{||}}{(2\pi)^{d-2}}\left[\ln\left(k_{||}^2 + k_{\perp\, cmn}^2\right) - \ln\left(k_{||}^2 + k_{0\perp\, mn}^2\right)\right] ,\end{aligned} \tag{21}$$

where $k_{0\perp\, mn}^2$ are the eigenvalues of the free operator in a box, with $\mu(\rho)$ set to zero. Color polarizations with $\alpha_c = 0$ do not contribute since at $\alpha_c = 0$ eq. (19) reduces to the free one.

We first integrate over $k_{||}$. In the $3d$ case the integration is finite:

$$\int_{-\infty}^{\infty}\frac{dk_{||}}{2\pi}\ln\left(\frac{k_{||}^2 + k_\perp^2}{k_{||}^2 + k_{0\perp}^2}\right) = |k_\perp| - |k_{0\perp}|. \tag{22}$$

In the $4d$ case integration over $k_{||}$ needs to be regularized. We use the Pauli–Villars regularization scheme, so that henceforth $\Lambda_{\rm QCD} = \Lambda_{P.V.} = e^{1/12}\Lambda_{\overline{MS}}$. We have

$$\int \frac{d^2k_{||}}{(2\pi)^2}\ln\frac{(k_{||}^2 + k_\perp^2)(k_{||}^2 + k_{0\perp}^2 + M^2)}{(k_{||}^2 + k_{0\perp}^2)(k_{||}^2 + k_\perp^2 + M^2)} = \frac{1}{4\pi}\left[k_\perp^2\left(\ln\frac{M^2}{k_\perp^2} + 1\right) - k_{0\perp}^2\left(\ln\frac{M^2}{k_{0\perp}^2} + 1\right)\right]. \tag{23}$$

There is a general formula for summation of any function of eigenvalues becoming continuous in the limit when the box radius goes to infinity, see Section 6. In the continuum limit the summation can be replaced by integration over the spectrum with a weight being the phase shift $\delta(k_\perp)$ of the corresponding differential equation, in this case eq. (19):

$$\sum_n \left[F(k_n) - F(k_{0n})\right] = -\frac{1}{\pi}\int_0^\infty dk\,\delta(k)\frac{dF(k)}{dk} \tag{24}$$

(the subscript $\perp$ will be henceforth suppressed). We shall describe the method of finding the phase shifts in Section 6. The phase shifts $\delta(k)$ depend on the 'partial wave' $m$ and on the color polarization $c$. Let us introduce the accumulated phase shift, summing over all partial waves,

$$\delta_c(k) = 2\sum_{m=1}^{\infty}\delta_{cm}(k) + \delta_{c0}(k). \tag{25}$$

Since $\alpha_c$ assumes as many "plus" values as there are "minus" ones, it is sufficient to sum over non-negative values of $m$. [Alternatively, one can take only positive values of $\alpha_c$ but then sum over all $m$'s, positive and negative.] Using the linearity of eq. (24) in $\delta(k)$ one can introduce the aggregate phase shift of the ghost operator,

$$\delta_{\rm ghost}(k) = \sum_c \delta_c(k). \qquad (26)$$

It is a common function both for $3d$ and $4d$. However, the expression for the ghost energy is different in $3d$ and $4d$, as the weights with which eigenvalues are taken are different, cf. eqs. (22,23). Using the general eq. (24) we obtain the needed transverse energy of the vortex as due to the ghost part of the quantum action :

$$\mathcal{E}^{3d}_{\rm ghost} = \frac{1}{\pi}\int_0^\infty dk\,\delta_{\rm ghost}(k) \qquad (27)$$

$$\mathcal{E}^{4d}_{\rm ghost} = \frac{1}{\pi^2}\int_0^\infty dk\,k\,\ln\frac{M}{k}\,\delta_{\rm ghost}(k). \qquad (28)$$

### C. The gluon operator

We now consider the gluon operator $W^{ab}_{\mu\nu}$, see eq. (13). Its $(D^2)^{ab}\delta_{\mu\nu}$ part is essentially identical to the ghost operator. For the other part we find the following eigenvalues:

$$\mathrm{Eig}(F^c_{\mu\nu}f^{acb}) = \frac{\mu'(\rho)}{\rho}(\{\alpha_c\}_{\rm color}\otimes\{\beta_\lambda\}_{\rm space}), \qquad \beta_\lambda = \begin{cases} \{0,1,-1\} & \text{for 3d,} \\ \{0,0,1,-1\} & \text{for 4d,} \end{cases} \qquad (29)$$

where the color eigenvalues $\alpha_c$ are the same as for the ghost operator, see eq. (18).

Therefore, the transverse eigenvalues $k_\perp$ of the gluon operator are found from solving the differential equation for the eigenfunctions $Z^{(c,\lambda)}_m(k_\perp\rho)$ where $c = 1,...,(N_c^2-1)$ labels the color polarization and $\lambda = 1,...,d$ labels the space polarization of the gluon:

$$\left[-\frac{1}{\rho}\frac{\partial}{\partial\rho}\rho\frac{\partial}{\partial\rho} + \frac{(m-\alpha_c\,\mu(\rho))^2}{\rho^2} - \frac{2\alpha_c\,\beta_\lambda\,\mu'(\rho)}{\rho}\right] Z^{(c,\lambda)}_m(\rho) = k^2_{\perp\,c\lambda m} Z^{(c,\lambda)}_m(\rho). \qquad (30)$$

According to eq. (15), the gluon contribution to the transverse energy of the vortex is the sum of logarithms of the eigenvalues:

$$\mathcal{E}_{\rm gluon} = \frac{1}{2}\sum_{c,\lambda,m,n,k_{||}}\left[\ln E^2(c,\lambda,m,n,k_{||}) - \ln E_0^2(c,\lambda,m,n,k_{||})\right]. \qquad (31)$$

Color polarizations with $\alpha_c = 0$ cancel from this equation. In $4d$ there are two space polarizations with $\beta_\lambda = 0$ for which the eigenvalue equation (30) reduces to that of the ghost operator, eq. (19). Therefore, $\mathcal{E}_{\rm ghost}$ is completely canceled by that part of the gluon operator spectrum. In $3d$ there is only one space polarization with $\beta_\lambda = 0$, so that the cancellation is not complete.

Similar to the previous subsection, we introduce the phase shifts $\delta(k)$ but now corresponding to eq. (30):

$$\delta^{(d)}_{\rm gluon}(k) = \sum_c\sum_\lambda \delta_{c\lambda}(k), \qquad \delta_{c\lambda}(k) = 2\sum_{m=1}^\infty \delta_{c\lambda m}(k) + \delta_{c\lambda 0}(k). \qquad (32)$$

Notice that, unlike the ghost case, here the aggregate phase shift depends on the number of dimensions as the number of gluon polarizations $\lambda$ is $d$-dependent. Using the results of the $k_{||}$ integration from the previous subsection we can write down the gluon contribution to the transverse energy via the aggregate phase shifts:

$$\mathcal{E}^{3d}_{\rm gluon} = -\frac{1}{2\pi}\int_0^\infty dk\,\delta^{(3)}_{\rm gluon}(k), \qquad (33)$$

$$\mathcal{E}^{4d}_{\rm gluon} = -\frac{1}{2\pi^2}\int_0^\infty dk\,k\,\ln\frac{M}{k}\,\delta^{(4)}_{\rm gluon}(k). \qquad (34)$$

### D. Full quantum energy

Adding up the ghost and gluon contributions to the quantum energy we get:

$$\mathcal{E}^{3d}_{\rm quant} = \frac{1}{\pi}\int_0^\infty dk \left[\delta_{\rm ghost}(k) - \frac{1}{2}\delta^{(3)}_{\rm gluon}(k)\right], \tag{35}$$

$$\mathcal{E}^{4d}_{\rm quant} = \frac{1}{\pi^2}\int_0^\infty dk\, k\, \ln\frac{M}{k} \left[\delta_{\rm ghost}(k) - \frac{1}{2}\delta^{(4)}_{\rm gluon}(k)\right]. \tag{36}$$

The combination of ghost and gluon phase shifts in the square brackets will be called the full phase shift; for various cases they are plotted in Figs. 2,4 and 5.

### E. Scaling properties

Let as assume that we have calculated the ghost and gluon phase shifts for a certain profile function $\mu(\rho/\rho_0)$ with $\rho_0 = 1$ in some arbitrarily chosen units. If we now change $\rho_0$ all quantities have to scale in accordance with the dimensional analysis of Section 4. Equations for $\mathcal{E}^{3d,4d}_{\rm quant}$ of the previous subsection can be translated into the following expressions for the constants $A, B, C$ introduced in Section 4:

$$A = \pi\rho_0^2 \int_0^\infty \frac{d\rho}{\rho}(\mu'(\rho))^2, \tag{37}$$

$$C = \frac{\rho_0}{\pi}\int_0^\infty dk \left[\frac{1}{2}\delta^{(3)}_{\rm gluon}(k) - \delta_{\rm ghost}(k)\right], \tag{38}$$

$$\tilde{A} = \frac{24\,\rho_0^2}{11\,N}\int_0^\infty dk\, k \left[\frac{1}{2}\delta^{(4)}_{\rm gluon}(k) - \delta_{\rm ghost}(k)\right], \tag{39}$$

$$\ln B = -\frac{1}{\tilde{A}}\frac{24\,\rho_0^2}{11\,N}\int_0^\infty dk\, k\, \ln(k\rho_0) \left[\frac{1}{2}\delta^{(4)}_{\rm gluon}(k) - \delta_{\rm ghost}(k)\right]. \tag{40}$$

As discussed in Section 4, the renormalizability of Yang–Mills theory in $4d$ requires that $\tilde{A} = A$: if that is satisfied the effective action does not depend on the ultraviolet cutoff $M$. This relation is, therefore, an important check of the numerics. It can be said that the calculation of $\tilde{A}$ is a particular way of getting numerically the '11/3' of the asymptotic freedom law. Further on, we verify the scaling relations (9,11) explicitly by changing the scale $\rho_0$ of the trial functions and checking that $\tilde{A}, B, C$ are $\rho_0$-independent.

Another powerful check of our numerical performance is provided by the number of colors $N$: the quantities $\tilde{A}$ and $B$ should be independent of $N$ while $C$ must be proportional to $N$. The calculations successfully pass these tests for the $\tilde{A}$ and $C$ within small errors, whereas the sensitivity of $B$ on the numerics is considerably larger, see Table I.

## VI. THE PHASE SHIFT METHOD

The $Z(2)$ vortex field $\mu(\rho)$ with $\mu(0) = 0$ and $\mu(\infty) = 1$ is very specific from the point of view of differential eqs. (19,30). Near the origin $\rho \approx 0$ the equations resemble the free equation for the Bessel functions $J_m(k\rho)$ while at infinity $\rho \to \infty$ they resemble the equation for $J_{m\pm1}(k\rho)$, with a shifted index. This is the essence of quantized $Z(2)$ vortices, see in this respect ref. [7].

This fundamental property of $Z(2)$ vortices causes certain difficulties in finding the continuous spectrum of eigenvalues in a given $m$ sector. We present here an economical method of dealing with this problem; it enables one to find the spectrum unambiguously. We have borrowed the idea of the method from Jost scattering theory, generalizing it to problems with cylindrical symmetry.

In the following we consider a general differential equation

| | $\mu(\rho)=\exp(-\rho_0/\rho-\rho/\rho_0)$ | | $\mu(\rho)=\exp(-(\rho_0/\rho)^3)$ | | $\mu(\rho)=(\rho/\rho_0)^6/((\rho/\rho_0)^6+1)$ | |
|---|---|---|---|---|---|---|
| | $\rho_0=1$ | $\rho_0=\sqrt{2}$ | $\rho_0=1$ | $\rho_0=\sqrt{2}$ | $\rho_0=1$ | $\rho_0=\sqrt{2}$ |
| $A$ | 0.2424 | 0.2424 | 2.2333 | 2.2333 | 3.3767 | 3.3767 |
| $N_c=2$: | | | | | | |
| $A/\tilde{A}$ | 1.0603 | 1.0066 | 1.0007 | 0.9862 | 1.0155 | 1.0026 |
| $B$ | 1.1686 | 1.0692 | 1.0388 | 1.0204 | 0.8854 | 0.8923 |
| $C$ | 0.1094 | 0.1089 | 1.1651 | 1.1513 | 1.5025 | 1.4693 |
| $N_c=3$: | | | | | | |
| $\frac{\tilde{A}(N_c=2)}{\tilde{A}(N_c=3)}$ | 1.0000 | 0.9999 | 1.0293 | 1.0331 | 1.0107 | 1.0193 |
| $\frac{B(N_c=2)}{B(N_c=3)}$ | 1.0082 | 1.0075 | 0.8767 | 0.8750 | 0.8751 | 0.8747 |
| $\frac{C(N_c=2)}{C(N_c=3)}$ | 0.6774 | 0.6766 | 0.6484 | 0.6511 | 0.6388 | 0.6387 |

TABLE I: Results for flux-0 and flux-1 profiles used. The table shows two columns for each profile one for $\rho_0 = 1$ and one for $\rho_0 = \sqrt{2}$.

$$\left[-\frac{1}{\rho}\frac{\partial}{\partial\rho}\rho\frac{\partial}{\partial\rho}+\frac{m^2}{\rho^2}+U(\rho)\right]Z(\rho)=k^2Z(\rho), \tag{41}$$

the equation for ghosts (19) and for gluons (30) being exactly of that form.

One looks for the solution which is regular at the origin and follows the oscillatory asymptotics of the Bessel function at infinity:

$$Z(r)=\sqrt{\frac{2}{\pi k\rho}}\cos\left[k\rho-\frac{\pi}{4}-\frac{m\pi}{2}+\delta(k)\right]. \tag{42}$$

This serves a definition of the phase shift $\delta(k)$. If the system is put in the box of large radius $R$ the zeros of (42) define the spectrum:

$$k_n=k_{0n}-\frac{\delta(k_n)}{R},\qquad k_{0n}=\frac{\pi}{R}\left(n+\frac{3}{4}+\frac{m}{2}\right) \tag{43}$$

where $k_{0n}$ is the spectrum with zero potential. A sum of any function of the eigenvalues $k_n$ in the continuum limit $(R\to\infty)$ becomes:

$$\sum_n\left[F(k_n)-F(k_{0n})\right]=-\frac{1}{R}\sum_n F'(k_n)\delta(k_n)=-\frac{1}{\pi}\int_0^\infty dk\,F'(k)\delta(k). \tag{44}$$

This is eq. (24) used in the previous section.

In the free case $(U=0)$ the differential eq. (41) have regular solutions $J_m(k\rho)$ (the ordinary Bessel functions), as well as singular solutions $Y_m(k\rho)$ (v.Neumann functions). From those one combines Hankel functions,

$$H_m^{\pm}(k\rho)=J_m(k\rho)\pm iY_m(k\rho). \tag{45}$$

Taking into account that $J_m$ and $Y_m$ are both solutions of the same differential equation, their Wronskian is a constant:

$$W(J_m,Y_m) \equiv k\rho\left[J_m(k\rho)Y'_m(k\rho) - J'_m(k\rho)Y_m(k\rho)\right] = \frac{2}{\pi}. \tag{46}$$

Using (46) one can easily verify that the needed solution $Z_m(k\rho)$ of eq. (41) satisfies the integral equation:

$$\begin{aligned} Z_m(k\rho) &= J_m(k\rho) - \frac{\pi}{2}\int_0^\rho d\rho'\rho'\left[J_m(k\rho)Y_m(k\rho') - J_m(k\rho')Y_m(k\rho)\right]U(\rho')Z_m(k\rho') \\ &= \mathrm{Im}\left\{iH_m^{(+)}(k\rho)\left[1 - \frac{i\pi}{2}\int_0^\rho d\rho'\rho' H_m^{(-)}(k\rho')U(\rho')Z_m(k\rho')\right]\right\} \\ &= \mathrm{Re}\left\{H_m^{(+)}(k\rho)\left[1 - \frac{i\pi}{2}\int_0^\rho d\rho'\rho' H_m^{(-)}(k\rho')U(\rho')Z_m(k\rho')\right]\right\}. \end{aligned} \tag{47}$$

It enables one to find $Z_m(k\rho)$ iteratively knowing the function at smaller values of $\rho$, starting from $\rho = 0$.

At $\rho \to \infty$ one obtains the asymptotics:

$$A\cos\left[k\rho - \frac{\pi}{4} - \frac{m\pi}{2} + \delta(k)\right] = \mathrm{Re}\left(e^{i(k\rho-\pi m/2-\pi/4)}\left[1 - \frac{i\pi}{2}\int_0^\infty d\rho'\rho' H_m^{(-)}(k\rho')U(\rho')Z_m(k\rho')\right]\right). \tag{48}$$

Putting $k\rho - m\pi/2 - \pi/4 = 2n\pi$ or $k\rho - m\pi/2 - \pi/4 = (2n+1/2)\pi$ with $n$ being a large integer and comparing the expressions we obtain the equation for the phase shift:

$$\tan\delta(k) = \frac{\mathrm{Im} f_m(k)}{\mathrm{Re} f_m(k)}, \qquad f_m(k) = 1 - \frac{i\pi}{2}\int_0^\infty d\rho\rho H_m^{(-)}(k\rho)U(\rho)Z_m(k\rho)\ . \tag{49}$$

We shall refer to eq. (49) as Jost equation as it is closely related to the theory of Jost functions developed in scattering theory, see e.g. [9].

We performed a numerical check of eq. (49) by taking, as an example, the potential arising from the gluon operator (see eq. (30)),

$$U(\rho) = \frac{1}{\rho^2}\left[(m - \alpha\mu(\rho))^2 - m^2 - 2\alpha\beta\rho\mu'(\rho)\right], \quad \text{with} \quad \mu(\rho) = \exp(-\rho - 1/\rho). \tag{50}$$

We computed the phase shifts directly from the shift of zeros of $Z_m(k\rho)$ with respect to those of the free $J_m(k\rho)$, and then compared with phase shifts obtained from eq. (49). The comparison of the two methods is shown in Fig. 1: the agreement is excellent. It is also seen that $\delta_m(k)$ decays fast as function of $m$.

One can simplify the method of finding the phase shifts even further. The second integration in eq. (49) is in fact unnecessary. Indeed, from eq. (47) one has the identity:

$$Z_m(k\rho) = \frac{1}{2}\left[H_m^{(+)}(k\rho)f_m(k) + H_m^{(-)}(k\rho)f_m^*(k)\right]. \tag{51}$$

Putting it in the Wronskian (see the definition (46)) we get:

$$W(Z_m, H_m^{(-)}) = \frac{1}{2}f_m(k)\ W(H_m^{(+)}, H_m^{(-)}) = if_m(k)\ W(Y_m, J_m) = -\frac{2i}{\pi}f_m(k). \tag{52}$$

Therefore the needed phase shift can be found directly from the Wronskian composed from the solution $Z_m(k\rho)$ and the Hankel function:

$$\delta_m(k) = \mathrm{Arg}(f_m(k)) = \mathrm{Arg}\left[\frac{i\pi}{2}W\left(Z_m, H_{|m|}^{(-)}\right)\right]. \tag{53}$$

Here $\mathrm{Arg}(re^{i\delta}) = \delta$ is the argument of a complex number. Notice that eq. (53) is independent of $\rho$. Therefore, evaluating the Wronskian in eq. (52) at different values of $\rho$ is a valuable check of the stability of the numerics. In fact, this method proves to be quite stable; we actually use it to calculate the phase shifts.

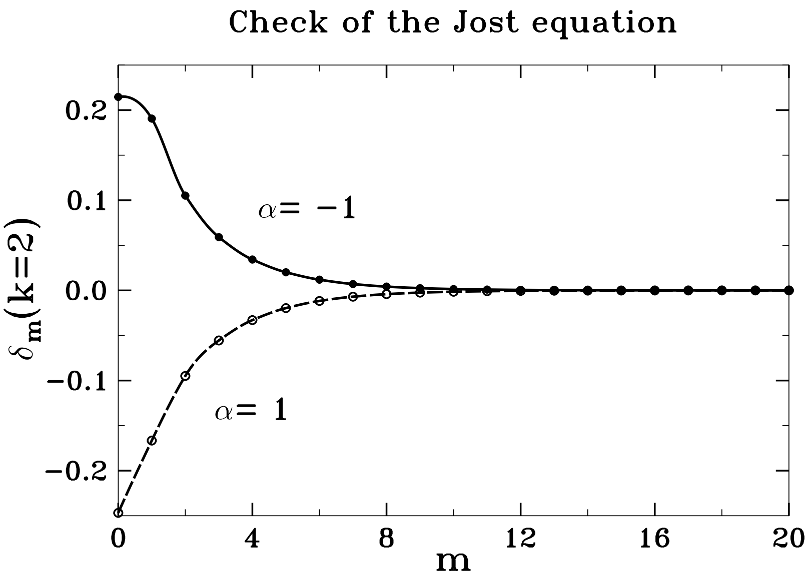


FIG. 1: Check of eq. (49). For $k = 2$, $\alpha = \pm 1$ and $\beta = 1$ we show the phase shift as function of $m$. The solid and dashed line present the phase shifts as obtained by extrapolating the difference of the zeros, while the open and filled circles show the result as obtained from eq. (49). One finds perfect agreement between the two methods. It is furthermore seen that the phase shifts decay rapidly in $m$.

## VII. RESULTS

### A. Flux-0 vortices

We first consider not a $Z(2)$ but a zero-flux vortex with $\mu(0) = \mu(\infty) = 0$. For definiteness we take a smooth profile of the form:

$$\mu(\rho) = \exp\left(-\rho - \frac{1}{\rho}\right). \tag{54}$$

Let us briefly describe the numerical procedure. We start by defining a range $R$ for a given value of $k$ and $m$ up to which the differential equations have to be solved. To make sure that we are working in an asymptotic regime we choose $R_{\max} = \max(60.0, x_{|m|15})/k$ where $x_{|m|n}$ is the $n$-th zero of the Bessel function $J_{|m|}(x)$. We have checked that for this choice the phase shifts calculated from eq. (49) and from eq. (53) do agree so that we are indeed reaching the asymptotic regime.

The initial condition for finding a regular solution $Z_m(\rho)$ is the free Bessel function which behaves as $J_m(k\rho) \approx (k\rho/2)^m/\Gamma(m+1)$ at small $\rho$: it is very small at large $m$. Therefore, for small $\rho$ (actually starting from some finite but small $\rho_{\min} = 0.00001/k$ and for $m \geq 4$) we solve, instead of eq. (41), the corresponding equation for the function $B(\rho) = Z(\rho)/((\rho/2)^m/\Gamma(m+1))$,

$$B''(\rho) = -B'(\rho)\frac{2m+1}{\rho} + \frac{B(\rho)((m - \alpha\mu(\rho))^2 - m^2 - 2\alpha\beta\rho\mu'(\rho))}{\rho^2} - k^2 B(\rho)\ . \tag{55}$$

with the initial conditions

$$B(\rho_{\min}) = 1, \qquad B'(\rho_{\min}) = -k\frac{k\rho_{\min}}{2(m+1)}\left(1 - \frac{(k\rho_{\min})^2}{4(m+2)}\right). \tag{56}$$

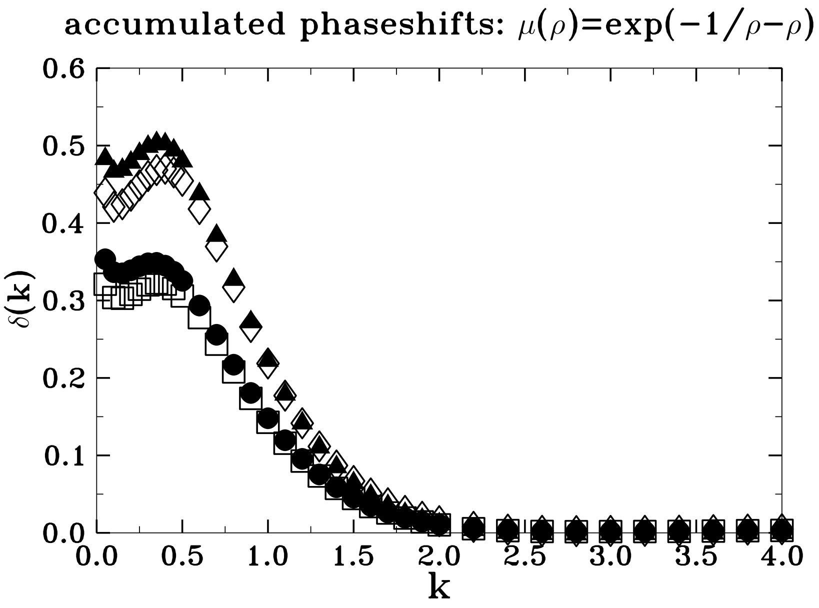


FIG. 2: Full phase shifts $\delta = \frac{1}{2}\delta_{\rm gluon} - \delta_{\rm ghost}$ for the profile $\mu(\rho) = \exp(-1/\rho - \rho)$: $\delta^{(3d)}_{N=2}(k)$ (filled circles), $\delta^{(3d)}_{N=3}(k)$ (filled triangles), $\delta^{(4d)}_{N=2}(k)$ (open squares), $\delta^{(4d)}_{N=3}(k)$ (open diamonds).

This differential equation is solved up to the point $R_p = 0.9x_{|m|1}/k$ where $x_{|m|1}$ is the first zero of the corresponding Bessel function. Starting from this point the original differential eq. (41) is solved, with the initial conditions:

$$\begin{aligned} Z(R_p) &= \frac{B(R_p)}{\Gamma(m+1)}\left(\frac{kR_p}{2}\right)^m \\ Z'(R_p) &= \frac{B'(R_p)}{\Gamma(m+1)}\left(\frac{kR_p}{2}\right)^m + \frac{kB(R_p)}{2\Gamma(m)}\left(\frac{kR_p}{2}\right)^{m-1} . \end{aligned}$$

We have checked that this procedure reproduces the usual Bessel functions in the free case, when $\mu(\rho) = 0$.

Having found the regular solution $Z_m(\rho)$, we use it to calculate phase shifts in three different ways. The first method is to use eq. (49), where the integration goes up to $R_{\rm max}$. This procedure becomes sometimes unstable because for large $\rho$ the integrand is oscillating. The two other methods exploit eq. (53). We evaluate the Wronskian either at $0.8R_{\rm max}$ or at $0.9R_{\rm max}$. We have checked that except in cases where the phase shift is consistent with zero these three different methods agree with each other. The phase shifts actually used in the results are the ones taken from the Wronskian evaluated at $0.8R_{\rm max}$.

The individual phase shifts at given $k$ are then accumulated over $m$, $c$ and $\lambda$. Fig. 2 shows the total aggregate phase shifts for N=2,3 in three and four dimensions. It is seen that in all cases $\delta(k)$ goes to zero quite fast for large $k$. For very small $k$ values $\delta(k)$ rises again after a maximum at $k = 0.4$

The results are shown in Table I. The $A$ coefficients of the classical and the quantum parts are equal within a small error due to the numerics, as it should be in order to ensure that in four dimensions the results are independent of the UV cutoff $M$. It is also seen that the $A$ coefficients are independent of the number of colors.

As a final step we check the scaling behavior predicted by eqs. (9,11). To that end we perform the same calculation again but for a profile $\mu(\rho) = \exp(-\sqrt{2}/\rho - \rho/\sqrt{2})$ and compare the result with the one obtained from the profile $\mu(\rho) = \exp(-1/\rho - \rho)$ and assuming the scaling eqs. (9,11). Tab. I shows indeed that in $3d$ and $4d$ the scaling law is fulfilled, which is yet another important cross check of our calculation. Furthermore, it is seen that in all cases we find a minimum of the effective action at negative values, which indicates that the vacuum is unstable against the production of zero-flux vortices. The values for the minima of the scaling factor are given in Table II.

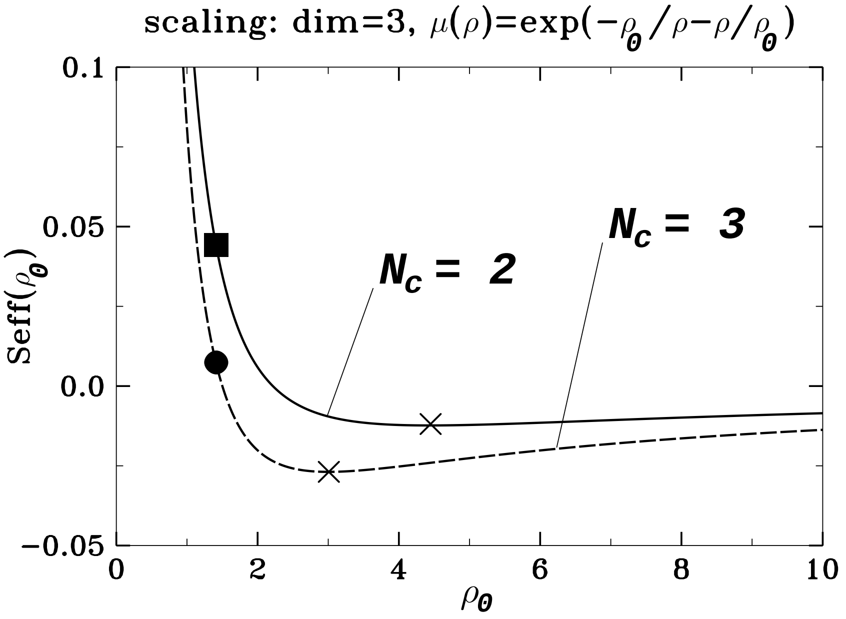


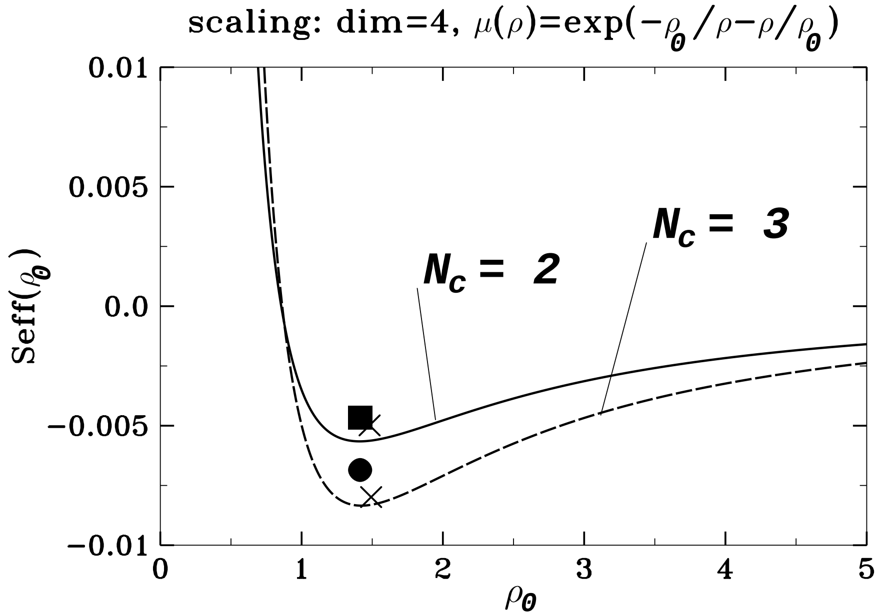


FIG. 3: Scaling behavior of the effective action in three and four dimensions: The figures show the effective action in three and four dimensions for the profile $\mu(\rho) = \exp(-\rho_0/\rho - \rho/\rho_0)$ as a function of $\rho_0$. The solid line shows the solution for $N_c = 2$ and the dashed line for $N_c = 3$. The dimensionfull constants have been set to 1, i.e. $g_3 = 1$ in three dimensions and $\Lambda_{\rm QCD} = 1$ in four dimensions. The filled circle and the square come from an independent calculation with $\rho_0 = \sqrt{2}$ explicitly plugged in. The crosses denote the place of the minimum of the effective action averaged over the results for $\rho_0 = 1$ and $\rho_0 = \sqrt{2}$, c.f. Table II.

### B. Flux-1 vortices

For the calculations with the $Z(2)$ unit-flux vortices we use the following trick which enables us to use the same technique as used for the flux-0 vortices. Instead of the actual flux-1 profile $\mu(\rho)$ with $\mu(0) = 0$ and $\mu(\infty) = 1$, we consider the profile $1 - \mu(\rho)$. From the energy point of view nothing is changed since the classical part depends only on the square of the first derivative of $\mu(\rho)$ while in the quantum part it corresponds to an overall shift of the summation in $m$. We have checked that in case of SU(2) this 'reflection' indeed produces the same results as if one makes the calculation directly with the flux-1 profile $\mu(\rho)$. For the $SU(2)$ vortex embedding into SU(3) this is not the case because here we have a contribution corresponding to the eigenvalues 1/2 in color space and the shift in integer units in the summation over $m$ does not work.

The numerics for the flux-1 vortices is more difficult than for the flux-0 ones. The first problem arises due to the fact that the phase shift exceeds $\pi$ in magnitude. As the arcus tangent is a multivalued function one then has to reconstruct the true function $\delta(k)$ by adding suitable multiples of $2\pi$ so that the resulting function is continuous in $k$. Furthermore, general constants in terms of suitable multiples of $\pi/4$ have to be added so that the aggregate phase shifts match each other for $k \to \infty$ at a value close to zero.

The second technical problem is that, literally speaking, $\delta(k)$ does not go to zero with $k \to \infty$, but rather approaches a small constant, see Figs. 4, 5. However, it seems to be a numerical artefact since, as one lowers $\rho_{\rm min}$ in eq. (56), the small constant becomes even smaller. Unfortunately, the numerical precision does not allow a complete annihilation of this spurious behavior. In fact, we have to make a cut at the point in k when the function becomes a (tiny) constant. The cross checks of renormalizability and the $N$ dependence are then fulfilled. We obtain for two different flux-1 profiles,

$$\begin{aligned} \mu^{(1)}(\rho) &= \exp(-1/\rho^3), \\ \mu^{(2)}(\rho) &= \rho^6/(\rho^6+1), \end{aligned} \tag{57}$$

the values of the coefficients in the effective action as given in Table I and Table II. The cross checks of renormalizability and N-dependence are fulfilled up to 5% as seen from Table I. Again in all cases the effective action exhibits a minimum. In all cases the minima are at negative values of the effective action, which means that the YM vacuum is unstable against the production of center vortices in the case of SU(2) in three and four dimensions and that it is even unstable with respect to the production of the embedding of center vortices in SU(3). Comparing the two profiles used it is seen that the power-like profile $\mu^{(2)}$ gives a slightly deeper minima than the exponential-like profile $\mu^{(1)}$.

## VIII. SUMMARY AND OUTLOOK

We have calculated the energy of quantum fluctuations (gluon and ghost) about vortices of various profiles. We have expressed the energy of quantum fluctuations through the phase shifts of the appropriate differential operators and developed and used an economical method to find the phase shifts, which is similar to that used in Jost's scattering theory.

Our results surpass many consistency tests. In $4d$ we actually manage to calculate numerically and with a good accuracy the "11/3" of the asymptotic freedom law; as a result we get the 'transmutation of dimensions' and express the vortex transverse size and transverse energy in terms of $\Lambda_{\overline{MS}}$, see Table I. This result is actually a powerful and non-trivial test of numerical precision. Explicit calculations with different transverse sizes confirm the natural behavior of quantum energy, which follows from dimensions.

The effective transverse energy of a vortex (classical plus quantum) has a minimum *lower* than the perturbative vacuum. It suggests that the vacuum is unstable with respect to the spontaneous production of center vortices. Vortex creation can be, in principle, stabilized by i) kinetic energy of vortex bending, ii) repulsive interaction of neighbor vortices and/or of different segments of the same vortex. However, at the moment we would be cautious to qualify our results as a direct evidence in favor of the 'entangled spaghetti' scenario, see the discussion in the Introduction. We have to add to the scepticism that zero-flux vortices which have no effect on the Wilson loops, also lead to a gain in energy just as the $Z(2)$ vortices do.

We did not attempt to find the absolute minimum of the effective action but restricted ourselves to a few concrete functional forms of the profile. Despite somewhat different shapes of the vortex profiles considered (one exponential,

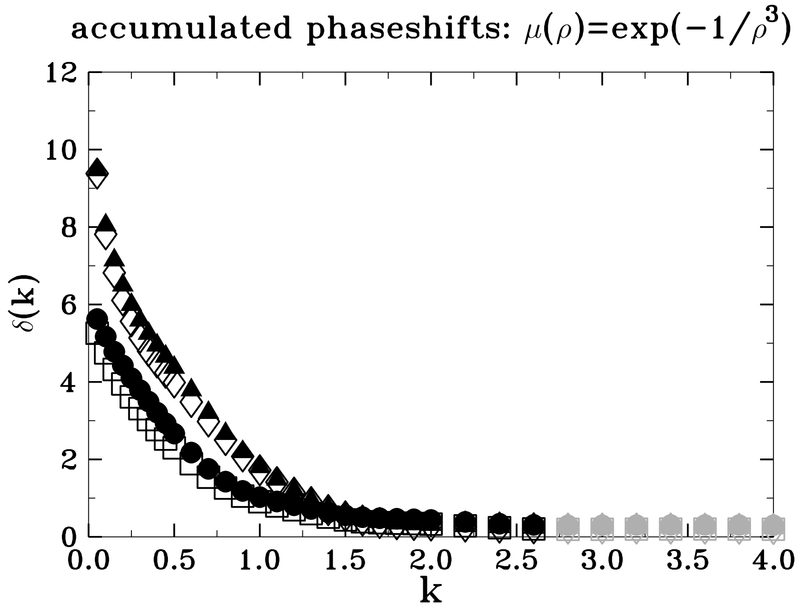


FIG. 4: Full phase shifts $\delta = \frac{1}{2}\delta_{\rm gluon} - \delta_{\rm ghost}$ for the profile $\mu(\rho) = \exp(-1/r^3)$: $\delta^{(3d)}_{N=2}(k)$ (filled circles), $\delta^{(3d)}_{N=3}(k)$ (filled triangles), $\delta^{(4d)}_{N=2}(k)$ (open squares), $\delta^{(4d)}_{N=3}(k)$ (open diamonds). The points in grey have been excluded from the analysis as the function $\delta(k)$ goes over to a spurious constant behavior.

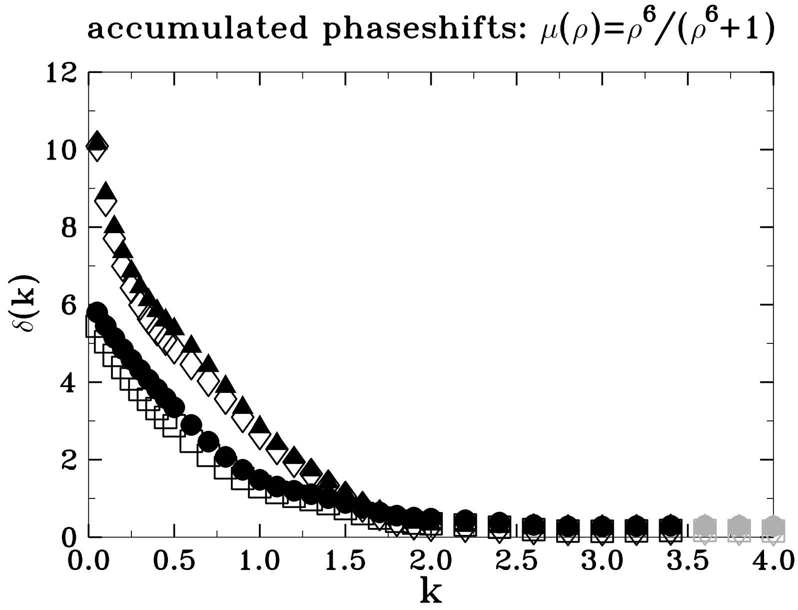


FIG. 5: Full phase shifts $\delta = \frac{1}{2}\delta_{\rm gluon} - \delta_{\rm ghost}$ for the profile $\mu(\rho) = \rho^6/(\rho^6+1)$: $\delta^{(3d)}_{N=2}(k)$ (filled circles), $\delta^{(3d)}_{N=3}(k)$ (filled triangles), $\delta^{(4d)}_{N=2}(k)$ (open squares), $\delta^{(4d)}_{N=3}(k)$ (open diamonds). The points in grey have been excluded from the analysis as the function $\delta(k)$ goes over to a spurious constant behavior.

| | $\mu(\rho) = \exp(-\rho_0/\rho - \rho/\rho_0)$ | $\mu(\rho) = \exp(-(\rho_0/\rho)^3)$ | $\mu(\rho) = (\rho/\rho_0)^6/((\rho/\rho_0)^6 + 1)$ |
|---|---|---|---|
| $N_c = 2$: | | | |
| $\rho^{(3d)}_{0\ \mathrm{min}}$ $[g_3^{-2}]$ | 4.441± 0.014 | 3.857± 0.032 | 4.546± 0.072 |
| $\mathcal{E}^{(3d)}_{\mathrm{min}}$ $[g_3^2]$ | -0.012± 0.000 | -0.150± 0.003 | -0.163± 0.005 |
| $\rho^{(4d)}_{0\ \mathrm{min}}$ $[\Lambda^{-1}]$ | 1.477 ± 0.093 | 1.601 ± 0.020 | 1.855 ±0.010 |
| $\mathcal{E}^{(4d)}_{\mathrm{min}}$ $[\Lambda^2]$ | -0.005 ± 0.001 | -0.040 ± 0.001 | -0.046 ± 0.000 |
| $N_c = 3$: | | | |
| $\rho^{(3d)}_{0\ \mathrm{min}}$ $[g_3^{-2}]$ | 3.007± 0.007 | 2.506± 0.028 | 2.903± 0.046 |
| $\mathcal{E}^{(3d)}_{\mathrm{min}}$ $[g_3^2]$ | -0.027± 0.000 | -0.356± 0.008 | -0.401± 0.013 |
| $\rho^{(3d)}_{0\ \mathrm{min}}$ $[\Lambda^{-1}]$ | 1.488 ± 0.093 | 1.403 ± 0.016 | 1.623 ± 0.009 |
| $\mathcal{E}^{(3d)}_{\mathrm{min}}$ $[\Lambda^2]$ | -0.008 ± 0.001 | -0.079 ±0.002 | -0.089 ± 0.001 |

TABLE II: Summary of the physical results with error bars. The physical result is the mean value from the two calculations at $\rho_0 = 1, \sqrt{2}$, while the error is given by the difference of these two values divided by the square root of two.

the other power-like) we get close numbers for the energy gain. It indicates that vortices are 'soft' with respect to their deformations in the transverse plane. A further indication in favor of this interpretation is the fast rise of the aggregate phase at small momenta, see Figs. 2,4,5, although zero modes in a strict sense do not seem to exist, see Appendix B. That makes the search for the absolute minimum rather senseless: it will be very flat anyhow. Simultaneously, it makes the naive interpretation of thick vortices as neatly shaped spaghetti even more difficult.

Concerning vortex interactions, a $Z(N)$ vortex in a regular gauge necessarily has a nonzero azimuthal component of the Yang–Mills field, decaying as $1/\rho$ at large distances from the center in the transverse plane. Two such vortices will then have unacceptable strong repulsion unless they are 'gauge-combed' in such a way that $A_\phi$ is zero at large distances. In such a gauge, however, one necessarily gets a Dirac sheet (in $3d$) or a Dirac volume (in $4d$) of gauge singularities. Dirac singularities from two vortices intersect along a line in $3d$ or along a surface in $4d$. An intersection of two gauge singularities in non-Abelian theory is, generally speaking, not a pure gauge but a physical singularity. It is not clear how to avoid those infinities. In any case, vortex interactions are far from being an easy topic, but they need to be clarified before the statistical mechanics of vortices can tell us that the 'entangled spaghetti' scenario has a preferred vacuum energy.

## APPENDIX A: CONVERSION INTO CYLINDRICAL COORDINATES

The conversion into cylindrical coordinates is given by the transformations:

$$x = \rho\cos\phi \qquad y = \rho\sin\phi \tag{A1}$$

and

$$\begin{aligned} A_x &= \cos\phi A_\rho - \sin\phi A_\phi \\ A_y &= \sin\phi A_\rho + \cos\phi A_\phi \end{aligned} \tag{A2}$$

$$\partial_x = \cos\phi\,\partial_\rho - \frac{\sin\phi}{\rho}\partial_\phi$$
$$\partial_y = \sin\phi\,\partial_\rho + \frac{\cos\phi}{\rho}\partial_\phi \ . \tag{A3}$$

One finds:

$$\begin{aligned} F_{12} &= \partial_x A_y - \partial_y A_x \\ &= \left(\cos\phi\,\partial_\rho - \frac{\sin\phi}{\rho}\partial_\phi\right)(\sin\phi A_\rho + \cos\phi A_\phi) \\ &\quad - \left(\sin\phi\,\partial_\rho + \frac{\cos\phi}{\rho}\partial_\phi\right)(\cos\phi A_\rho - \sin\phi A_\phi) \\ &= \frac{A_\phi}{\rho} + \frac{\partial A_\phi}{\partial\rho} \ , \end{aligned} \tag{A4}$$

using $A_\rho = 0$, and with $A_\phi = \mu(\rho)/\rho$ one obtains:

$$F_{12} = \mu'(\rho)/\rho \quad \Rightarrow \quad (F_{\mu\nu})^2 = 2[\mu'(\rho)/\rho]^2 \ . \tag{A5}$$

## APPENDIX B: EXCLUDING POSSIBLE BOUND STATES AT $k = 0$

The spectrum of the ghost and gluon operators discussed above is incomplete if there exist bound states at $k_\perp = 0$. Were the vortices an exact solution of the classical equation of motion, zero modes would be inevitable. However, our vortices are minima of the effective action and not of the classical one, therefore there are no special reasons for zero modes of the small-oscillation operators.

To check whether such states exist we substitute $\rho \to t = 1/\rho$ in the gluon operator and obtain the reflected differential equation:

$$-t\frac{\partial}{\partial t}t\frac{\partial}{\partial t}Z(1/t) + \left[(m - \alpha\mu(1/t))^2 + 2\alpha\beta\frac{\mu'(1/t)}{t}\right] Z(1/t) = 0 \ . \tag{B1}$$

$\alpha$ and $\beta$ are two constants depending on the color and space polarizations of the state under consideration. Using the notation B(t) = Z(1/t) we take the boundary conditions for a bound state $B(0) = 0$. This tells only that B has to be regular at the origin. Now we can check the asymptotic of the equation using an explicit flux-1 profile, for example, $\mu(\rho) = \exp(-1/\rho^3)$. One obtains asymptotically for large $\rho$ and correspondingly for small $t$:

$$\left[-\frac{1}{t}\frac{\partial}{\partial t}t\frac{\partial}{\partial t} + \frac{(m-\alpha)^2}{t^2}\right] B_0(t) = 0 \ . \tag{B2}$$

For this equation we require power series in $t$. The only non-trivial regular solution to this is $B_0(t) = At^{|m-\alpha|}$. Therefore, we use the ansatz:

$$B(t) = A(t)t^{|m-\alpha|} \ . \tag{B3}$$

One obtains the differential equation for the amplitude:

$$\left[-\frac{1}{t}\frac{\partial}{\partial t}t\frac{\partial}{\partial t} - 2\frac{|m-\alpha|}{t}\frac{\partial}{\partial t} + \frac{(m-\alpha\mu(1/t))^2 - (m-\alpha)^2 + 2\alpha\beta\mu'(1/t)/t}{t^2}\right] A(t) = 0 \ . \tag{B4}$$

The boundary conditions are now $A(0) = 1, A'(0) = 0$ to make sure that the asymptotical behavior is correct. Explicit calculation shows that these states behave as:

$$Z_m^{(\alpha,\beta)}(\rho) \sim \begin{cases} \rho^{-|m|} & \text{for small } \rho \\ \rho^{-|m-\alpha|} & \text{for large } \rho \end{cases} \quad \text{for } m > 0 \ . \tag{B5}$$

The behavior at small $\rho$ is clear because of asymptotic arguments like the one used for small $t$ in Eq. (B2). The explicit calculation shows that only irregular solutions exist for $m > 0$. In the case $m = 0$ the solution is at least logarithmically divergent for large $\rho$, as $|\alpha| = 1, 1/2$. Therefore, there are no localized solutions with zero $k_\perp$.

[1] G. 't Hooft, Nucl. Phys. **B138**, 1 (1978).
[2] M. Faber, J. Greensite and S. Olejnik, JHEP **0006**, 041 (2000) [arXiv:hep-lat/0005017].
[3] L. Del Debbio, M. Faber, J. Greensite and S. Olejnik, Phys. Rev. **D55** (1997) 2298 [arXiv:hep-lat/9610005].
[4] M. Engelhardt, H. Reinhardt, Nucl. Phys. **B585** (2000) 591.
[5] D. Diakonov and V. Y. Petrov, Nucl. Phys. **B245**, 259 (1984).
[6] D. Diakonov and M. Maul, Nucl. Phys. **B571**, 91 (2000) [arXiv:hep-th/9909078].
[7] D. Diakonov, Mod. Phys. Lett. **A14** (1999) 1725 [hep-th/9905084].
[8] D. Diakonov, V. Y. Petrov and A. V. Yung, Phys. Lett. **B130** (1983) 385.
[9] John R. Taylor, Scattering Theory: The quantum theory of non-relativistic collisions, Wiley, 1972, ISBN 0-471-84900-6.